

Low-Velocity Impacts on Scarf Joints

U.A. Khashaba¹, R. Othman^{2,3}, I.M.R. Najjar³

^{1,2,3} Mechanical Engineering Department, Faculty of Engineering, King Abdulaziz University, P.O. Box 80204, Jeddah 21589, Saudi Arabia

ARTICLE INFO

ABSTRACT

corresponding Author:

R. Othman

Associate Professor,
Mechanical Engineering
Department, Faculty of
Engineering, King
Abdulaziz University

Adhesive bonding is widely used in several engineering fields. During fabrication or manufacturing low-velocity impacts can occur. In this work, low-velocity impact resistance of adhesively bonded composite scarf joint is investigated. Two adhesives are considered: a neat epoxy and a carbon nanotube (CNT) doped epoxy. It is showed the MWCNT doping increases the strength of the joint. However, absorbed energy and deflection at failure are decreased.

KEYWORDS: *Scarf Joint; Low-velocity impact; Adhesion; Epoxy; Composites; Carbon Nanotubes*

I. INTRODUCTION

Nowadays, the use of composites in structural components is in continuous increase in several engineering fields such in automobile, railway, marine, and aeronautical engineering. These structural parts may face low-velocity impacts during fabrication or maintenance. If the impact energy is higher than a threshold value, the low-velocity impacts cause degradation or fracture of the composite structure.

Numerous works have assessed the impact damage resistance of composites plates to low-velocity impacts [1-]. Aymerich et al. [1-2] were interested on the damaged induced by low-velocity impacts on stitched and unstitched graphite/epoxy laminates. They considered impact energies ranging from 1 to 14 J. Moreover, they examined the damaged composite plates by x-ray analysis. This showed that damage is present as delamination and matrix cracks. They also showed that impact energies higher than 8 J caused fiber fracture. Dau et al. [3] delat with the impact damage resistance of 3D-interlock composites.

The impact or was made from Styrene Butadyene-Styrene and has a hemispherical shape. A high speed camera was employed to acquire photographs during the impact. These photographs

were analyzed using a digital image correlation (DIC) software. This allowed them to monitor the deformation of the composite plate. As 3D interlock composites has high resistance against delamination, the examined impact energies ranged between 202 J and 346 J. Evci and Gulgec [4] reported that impact damage area is more extended in the case of uni-directional composites than in the case of woven composites. Thus the fiber reinforcement geometry has a substantial effect on the impact damage resistance.

Multiple other parameters can affect the impact damage resistance of composite materials. Kursun et al. [5] investigated the influence of the effect of the drop-weight shape. The considered impact energies were between 29 and 45 J. Kostopulos et al. [6] studied the effects of doping CFRE composites by multi-wall carbon nano-tubes (MWCNT). They found that MWCNT doping leads to better CAI mechanical properties. The CAI strength is 10%-lower for the non-doped specimens than the neat composite plates than the doped ones. Iqbal et al. [7] were interested in the impact damage in CFRE reinforced with nanoclay fillers. Moreover, They studied the compression after impact (CAI) properties. They suggested that adding of 3% is the optimal with respect to the

damage resistance when compared to adding 0% or 5% of nanoclay fillers. Soliman et al. [8] observed that doping composite plates by 1.5% of multi-wall carbon nano-tubes leads to 50% improvement of the absorbed energy.

The fiber and matrix materials have also big influence on the impact damage resistance. Liang et al. [9] studied low-velocity impact flax/epoxy composite plates. They measured 15 to 30% drop of the compression strength at 10 J of impact energy. Recently, there an increasing interest in thermoplastic composite materials. Thus, low-velocity impact damage resistance of fiber reinforced ultra-high molecular polyethylene [10] and Kevlar/polypropylene composite plates [11] were recently reported in the literature.

In addition to the material parameters, environmental parameters have also strong effects as mainly the polymeric matrices are largely sensitive to temperature and water absorption. Khashaba and Othman [12] undertook low-velocity impact tests on CFRE at room temperature (RT), 50°C and 75°C. They observed that CAI properties are equivalent at room temperature and 50°C. CAI stiffness and strength are the lowest at 75°C. However, Suvarna et al. [13] reported that the damage area is larger and the after-impact flexural strength decreases as the impact temperature drops. Taraghi et al. [14] reported low-velocity impact tests on Kevlar/epoxy woven laminate composites at room and low temperatures. Kumar et al. [15] reported that peak force slightly drops if the temperature increases while studying hemp-basalt/epoxy composites. Aktas et al. [16] showed that CAI strength of glass/ epoxy composites drops as the temperature increases.

In terms of water absorption effects, Arun et al. [16] investigated the influence of sea water. They reported that the impact toughness decreases as the exposure duration to the sea water becomes longer. They were studying glass/textile fabric polymer hybrid composites. Yahaya et al. [18]

observed a substantial drop of CAI strength, because of water absorption, in woven kenaf-kevlar hybrid composites. Ahmad et al. [19-20] reported also a drop in penetration resistance of both orthotropic and unidirectional CFRP composites. Recently, Khashaba et al. [21] reported that the water absorption affects more the peak force than the absorbed energy while testing water-saturated and dry CFRE composite plates under low-velocity impacts.

There is a plentiful of researches who have dealt with the impact damage resistances of composite plates. In this work, we are interest in the low-velocity impact response of adhesively bonded scarf composite joints. Few works have studied the low-velocity impact response of composite joints. Very few of them investigated the impact response of scarf joints. Nie et al. [22-23] undertook low-velocity impact on composite scarf joints. They also carried out tensile-after-impact tests. They reported that the impact resistance and tensile-after-impact (TAI) is highly sensitive to the impact location. Harman and Wang [24] compared the low-velocity impact resistance of scarf joints to the parent uniform composite. They observed an increase in vulnerability of the scarf joint compared to the parent composite coupon. They recommended the use of a doubler which was showed to improve the damage tolerance. Takahashi et al. [25-26] investigated the low-velocity impact response of composite scarf joints with diverse stacking sequences and several scarf angles. They reported debonding for the all studied cases between the adhesive layer and the repaired composite laminate.

II. METHODOLOGY

A. *Materials and specimens*

In the present work, two groups of SAJs were fabricated from carbon fiber reinforced epoxy composite adherends and different adhesive materials. The adherends were assembled using neat epoxy adhesive and modified epoxy with optimum weight percentage of Multi-Walled

Carbon Nanotubes (MWCNTs).

The adherends of the scarf adhesive joints were cut from carbon fiber reinforced epoxy (CFRE) composite laminates with dimensions of 500x500x5 mm, which were fabricated using prepreg technique. The constituent materials, manufacturing technique and mechanical properties of CFRE composites are reported elsewhere by Khashaba et al. [27-30].

The used adhesive epoxy is Epocast 50-A1/946 manufactured by Huntsman Advanced Materials Americas Inc. The adhesive epoxy was modified with optimum weight percentage of 0.5 wt% Multi-Walled Carbon Nanotubes (MWCNTs) using sonication technique. Details about the epoxy adhesive, MWCNTs, sonication technique and the mechanical properties of epoxy adhesive (with and without MWCNTs) are presented earlier by Khashaba et al. [31-32].

The SAJs with taper (scarf) angle of 45° were cut to the dimensions shown in Fig. 1. Details about the machining of the taper surfaces of the adherends with scarf angle of 45°, preparing the machined tapered surfaces, preparing the adhesive materials and fabrication procedures of the SAJs are presented elsewhere by Khashaba et al. [27-30]. The tensile properties of the fabricated 45°-SAJ with and without MWNTs were presented earlier [29].

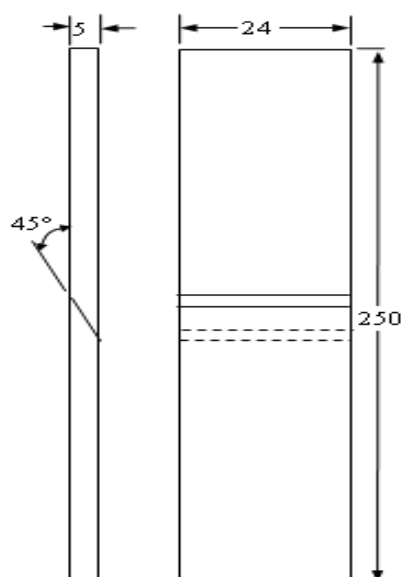


Fig. 1: Scarf adhesive joint dimensions

B. Impact testing

The scarf composite joints were subjected to low-velocity impacts using CEAST 9340 drop-weight impact testing machine as shown in Fig. 2.

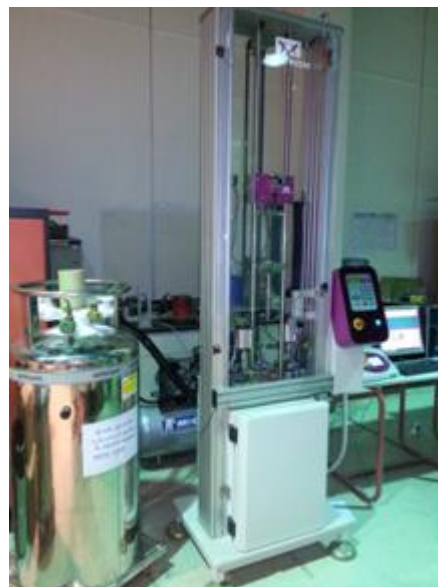


Fig. 2: CEAST 9340 drop-weight impact testing machine

The scarf composite joints were subjected to low-velocity impacts using CEAST 9340 drop-weight impact testing machine as shown in Fig. 2. Three specimens were tested for each type of adhesive. They were tested at room temperature. The scarf joints were double-camped. They were impact at an impact energy of 1.25 J. This corresponds to total impact mass of 3.132 kg (tup mass: 0.632 kg and tup holder mass: 2.5 kg). To achieve the impact energy of 1.25 J, the total mass was dropped from a height of 40.7 mm which leads to an impact velocity of 0.8934 m/s. A hemispheric impactor of 16 mm in diameter was used for these tests. In order to prevent any re-bounce, the drop-weight machine is equipped with an anti-rebound pneumatic system. The drop-weight testing machine is also equipped with a force sensor. For each test the impact force, $P(t)$, was measured. Knowing the force, it is possible to find the acceleration of the impactor, by applying Newton's second law. Namely,

$$a(t) = g - \frac{P(t)}{m}, \quad (1)$$

where $a(t)$, g and m are the impactor acceleration, gravity acceleration and impactor mass, respectively. Subsequently, the acceleration is integrated with respect of time to obtain the impactor velocity $v(t)$:

$$v(t) = v_i + \int_0^t \left(g - \frac{P(\tau)}{m} \right) d\tau, \quad (2)$$

where v_i is the impact velocity. A second integration yields the impactor displacement. More precisely,

$$u(t) = \int_0^t v(\tau) d\tau, \quad (3)$$

where $u(t)$ is the impactor displacement or also the scarf joint's deflection. As the load and the velocity are known, it is then possible to determine the energy transferred from the impactor to the scarf joints. Expressly,

$$E(t) = \int_0^t v(\tau)P(\tau) d\tau, \quad (4)$$

as the product $v(t)P(t)$ gives the instantaneous power.

In this work, we are interested in the time variation of the force, displacement and energy. However, we are mainly dealing with the value of the force, displacement and energy at the instant of failure: P_u , u_u and E_u , respectively. The subscript $_u$ is used for the word ultimate.

III. RESULTS AND DISCUSSION

A. Force vs. time

Fig. 3 shows the variation of the force in terms of time obtained with both the neat epoxy and the CNT doped epoxy as measured by the drop-weight testing machine. In the two studied cases, an elastic-brittle behavior of the adhesive is observed. Indeed, the force increases almost linearly (except for some oscillations) till a maximum value of the force. Subsequently, a sharp drop is observed corresponding to failure/ collapse of the scarf joint. The maximum force observed with the

CNT adhesive is higher than the one observed with the neat adhesive. Furthermore, the failure arrives faster in the case of the CNT adhesive. The failure for the neat adhesive takes more time to happen.

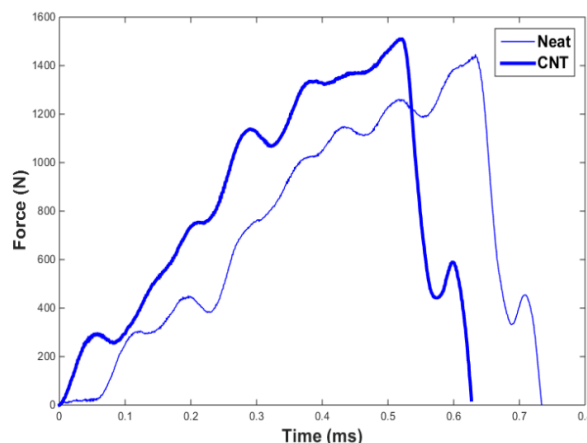


Fig. 3: Force vs. time for neat and CNT epoxies

B. Force vs. deflection

Fig. 4 shows the variation of the force in terms of the joint's deflection/impactor displacement. This curve confirms the elastic behavior of the joint before failure as the slope of curves is almost linear. The observed oscillations are caused by the excitation of the natural frequencies of the testing machine. The slope of the CNT doped joint is higher than the neat joint. Actually the CNT reinforces the adhesive and increases its stiffness. The neat adhesive is more flexible.

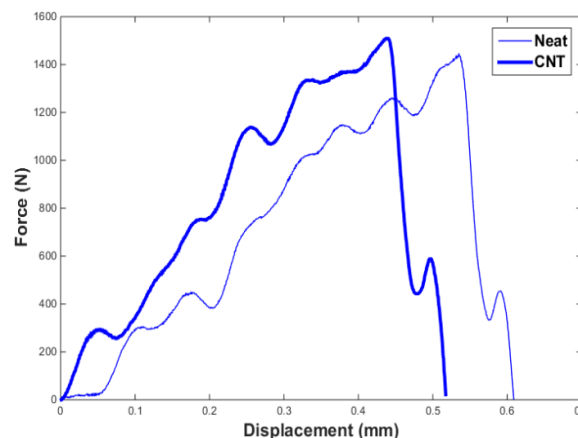


Fig. 4: Force vs. deflection/displacement for neat and CNT epoxies

C. Energy vs. deflection

Fig. 5 shows the variation of the energy in terms of the joint's deflection. The curves have a parabolic shape in the majority of the curve. This is due to the elastic behavior of the adhesive. Indeed, the energy can be written in this part of the curve as as:

$$E = \frac{1}{2}ku^2. \quad (5)$$

where k is the elastic stiffness of the joint. Once failure occurs, a slip to the right of the curve is observed.

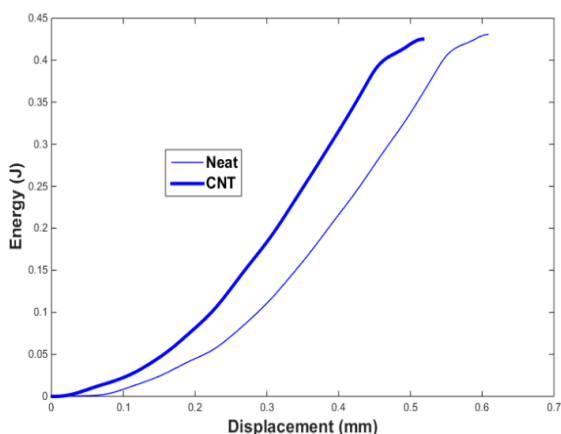


Fig. 5: Force vs. deflection/displacement for neat and CNT epoxies

D. Failure

The CNT doping reinforces the epoxy adhesive and its strength is increases. Thus, the maximum force (or force at failure) is higher with the CNT doping (Fig. 6). However, the CNT doping makes the adhesive more brittle. Hence, the maximum deflection (deflection at failure) is higher with the neat epoxy (Fig. 6). These two effects compete and as a result the absorbed energy is more important with the neat epoxy (Fig. 6).

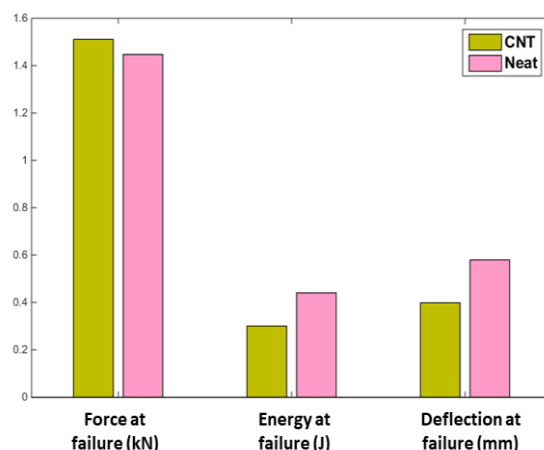


Fig. 6: Force, energy and deflection at failure for neat and CNT epoxies

IV. CONCLUSIONS

The low-velocity impact of scarf joint were studied. It is shown the CNT doping increases the strength of the adhesive and thus the force at failure. However, the CNT doping makes the adhesive more brittle. Consequently, the deflection at failure and the absorbed energy at higher with the neat epoxy adhesive.

ACKNOWLEDGMENTS

This work was funded by the Deanship of Scientific Research (DSR), King Abdulaziz University, Jeddah, under grant no. G-196-135-38. The authors, therefore, acknowledge with thanks DSR for technical and financial support.

REFERENCES

1. Aymerich F, Pani C, Priolo P. Damage response of stitched cross-ply laminates under impact loadings. *Eng Fract Mech* 2007; 74:500–14.
2. Aymerich F, Pani C, Priolo P. Effect of stitching on the low-velocity impact response of [03/903]s graphite/epoxy laminates. *Compos Part A* 2007; 38:1174– 82.
3. Dau F, Dano ML, Duplessis-Kergomard Y. Experimental investigations and variability considerations on 3D interlock

- textile composites used in low velocity soft impact loading. *Compos Struct* 2016; 153:369–79.
4. Evci C, Gulgec M. An experimental investigation on the impact response of composite materials. *Int J Impact Eng* 2012; 43:40–51.
 5. Kursun A, Senel M, Enginsoy HM, Bayraktar E. Effect of impactor shapes on the low velocity impact damage of sandwich composite plate: experimental study and modeling. *Compos B* 2016; 86:143–51.
 6. Kostopoulos V, Baltopoulos A, Karapappas P, Vavouliotis A, Paipetis A. Impact and after-impact properties of carbon fibre reinforced composites enhanced with multi-wall carbon nanotubes. *Compos Sci Technol* 2010; 70:553–63.
 7. Iqbal K, Khan SU, Munir A, Kim JK. Impact damage resistance of CFRP with nanoclayfilled epoxy matrix. *Compos Sci Technol* 2009; 69:1949–57.
 8. Soliman EM, Sheyka MP, Taha MR. Low-velocity impact of thin woven carbon fabric composites incorporating multi-walled carbon nanotubes. *Int J Impact Eng* 2012; 47:39–47.
 9. Liang S, Guillaumat L, Gning PB. Impact behaviour of flax/epoxy composite plates. *Int J Impact Eng* 2015; 80:56–64.
 10. Hazzard MK, Hallett S, Curtis PT, Iannucci L, Trask RS. Effect of fibre orientation on the low velocity impact response of thin Dyneema composite laminates. *Int J Impact Eng* 2017; 100:35–45.
 11. Bandaru AK, Chavan VV, Ahmad S, Alagirusamy R, Bhatnagar N. Low velocity impact response of 2D and 3D Kevlar/polypropylene composites. *Int J Impact Eng* 2016; 93:136–43.
 12. Khashaba UA, Othman R. Low-velocity impact of woven CFRE composites under different temperature levels. *Int J Impact Eng* 2017; 108: 191-204.
 13. Suvarna R, Arumugam V, Bull DJ, Chambers AR, Santulli C. Effect of temperature on low velocity impact damage and post-impact flexural strength of CFRP assessed using ultrasonic C-scan and micro-focus computed tomography. *Compos B* 2014; 66:58–64.
 14. Taraghi I, Fereidoon A, Taheri-Behrooz F. Low-velocity impact response of woven Kevlar/epoxy laminated composites reinforced with multi-walled carbon nanotubes at ambient and low temperatures. *Mater Des* 2014;53:152–8.
 15. Suresh Kumar C, Arumugam V, Dhakal HN, John R. Effect of temperature and hybridisation on the low velocity impact behavior of hemp-basalt/ epoxy composites. *Compos Struct* 2015; 125:407–16.
 16. Aktas M, Karakuzu R, Arman Y. Compression-after impact behavior of laminated composite plates subjected to low velocity impact in high temperatures. *Compos Struct* 2009; 89:77–82.
 17. Arun KV, Basavarajappa S, Sherigara BS. Damage characterisation of glass/textile fabric polymer hybrid composites in sea water environment. *Mater Des* 2010; 31: 930–9.
 18. Yahaya R, Sapuan SM, Jawaid M, Leman Z, Zainudin ES. Water absorption behaviour and impact strength of kenaf-kevlar reinforced epoxy hybrid composites. *Adv Compos Lett* 2016; 25: 89-102.
 19. Ahmad F, Abbassi F, Hong JW, Chang SH, Park MK. Hygroscopic effects on the penetration-resistance behavior of a specially-orthotropic CFRP composite plates. *Compos Struct* 2017, 176: 1073-80.
 20. Ahmad F, Hong JW, Choi HS, Park MK.

- Hygro effects on the low-velocity impact behavior of unidirectional CFRP composite plates for aircraft applications. *Compos. Struct.* 2016; 135: 276-85.
21. Khashaba UA, Othman R, Najjar IMR. Effect of Water Absorption on the Impact Behaviors of CFRE Composites. *Global J Res Eng A* 2017; 17(6): 41-48.
 22. Nie H, Xu J, Guan Z, Li Z, Ji Z, Tan R. Tensile behavior of scarf joints after impact in different locations. *Beijing Hangkong Hangtian Daxue Xuebao/ J Beijing Univ Aeronaut Astronaut* 2016; 42(11): 2306-20.
 23. Nie H, Xu J, Guan Z, Li Z. Tensile behaviors after impact of composite scarf joints. (2016) *Proceedings of 2016 7th International Conference on Mechanical and Aerospace Engineering, ICMAE 2016*, art. no. 7549500, pp. 9-16.
 24. Harman AB, Wang CH. Damage tolerance and impact resistance of composite scarf joints. *ICCM International Conferences on Composite Materials 2007*.
 25. Takahashi I, Takeda SI, Iwahori Y, Takeda N. Evaluation of the impact damages of scarf-repaired composites. *Zairyo/Journal of the Society of Materials Science* 2007; 56(5): 414-9.
 26. Takahashi I, Takeda SI, Iwahori Y, Takeda N. Evaluation of the impact damages of composites repaired by scarf technique. *Proceedings of the 12th U.S.-Japan Conference on Composite Materials 2006*; 155-169.
 27. Khashaba UA, Aljinaidi AA, Hamed MA. Fatigue and reliability analysis of nano-modified scarf adhesive joints in carbon fiber composites. *Compos. B* 2017; 120: 103–117
 28. Khashaba UA, Aljinaidi AA, Hamed MA. Development of CFRE composite scarf adhesive joints with SiC and Al₂O₃ nanoparticle. *Compos. Struct.* 128 (2015) 415–427.
 29. Khashaba UA, Aljinaidi AA, Hamed MA. Analysis of adhesively bonded CFRE composite scarf joints modified with MWCNTs. *Compos.* 2015; 71:59–71.
 30. Khashaba UA, Najjar IMR. Adhesive layer analysis for scarf bonded joint in CFRE composites modified with MWCNTs under tensile and fatigue loads. *Compos. Struct.* 2018;184:411–427
 31. Khashaba UA, Aljinaidi AA, Hamed MA. Nanofillers modification of Epocast 50-A1/946 epoxy for bonded joints. *Chin. J. Aeronaut.* 2014; 27:288–1300
 32. Khashaba UA. Improvement of toughness and shear properties of multi-walled carbon nanotubes/epoxy composites. *Polym. Compos.* 2017; In press. DOI: <http://dx.doi.org/10.1002/pc.24003>